ACS chemical biology

ARTICLE

Gene Silencing Activity of siRNAs with a Ribo-difluorotoluyl Nucleotide

Jie Xia[†], Anne Noronha[†], Ivanka Toudjarska[†], Feng Li[‡], Akin Akinc[†], Ravi Braich[†], Maria Frank-Kamenetsky[†], Kallanthottathil G. Rajeev[†], Martin Egli[‡], and Muthiah Manoharan[†,*]

[†]Alnylam Pharmaceuticals, Inc., 300 Third Street, Cambridge, Massachusetts 02142, and [‡]Department of Biochemistry, Vanderbilt University, School of Medicine, Nashville, Tennessee 37232

ABSTRACT Recently, chemically synthesized short interfering RNA (siRNA) duplexes have been used with success for gene silencing. Chemical modification is desired for therapeutic applications to improve biostability and pharmacokinetic properties; chemical modification may also provide insight into the mechanism of silencing. siRNA duplexes containing the 2,4-difluorotoluyl ribonucleoside (rF) were synthesized to evaluate the effect of noncanonical nucleoside mimetics on RNA interference. 5′-Modification of the guide strand with rF did not alter silencing relative to unmodified control. Internal uridine to rF substitutions were well-tolerated. Thermal melting analysis showed that the base pair between rF and adenosine (A) was destabilizing relative to a uridine-adenosine pair, although it was slightly less destabilizing than other mismatches. The crystal structure of a duplex containing rF○A pairs showed local structural variations relative to a canonical RNA helix. As the fluorine atoms cannot act as hydrogen bond acceptors and are more hydrophobic than uridine, there was an absence of a well-ordered water structure around the rF residues in both grooves. siRNAs with the rF modification effectively silenced gene expression and offered improved nuclease resistance in serum; therefore, evaluation of this modification in therapeutic siRNAs is warranted.

*To whom correspondence should be addressed.
E-mail: mmanoharan@alnylam.com.

Received for review February 4, 2006 and accepted April 10, 2006.

Published online April 17, 2006.

10.1021/cb600063p CCC: $33.50

Short interfering RNAs (siRNAs) are 21–23 nucleotides long RNA duplexes. One of the strands of the siRNA duplex, the guide (antisense) strand, is incorporated into a complex of enzymes called the RNA-induced silencing complex (RISC). The small RNA component serves as a guide to identify a complementary sequence in a messenger RNA (mRNA) and causes the mRNA to be cleaved by RISC or prevents it from being translated into protein (*1–4*). The result is that the targeted gene is silenced.

Although unmodified siRNA duplexes have been used with success for gene silencing, chemical modification of one or both of the strands is desired for therapeutic applications to enhance stability and to improve pharmacokinetic properties. Numerous chemical modifications have been evaluated, but only a few nucleobase modifications have been tested for effects on siRNA activity (*5–7*). It is not clear which of these nucleobase modifications are recognized and accepted by the RNA-induced silencing complex, RISC, during the course of RNA interference.

The 2′-deoxydifluorotoluyl nucleoside (dF) is a nonpolar nucleoside analogue invented by Kool and co-workers that is an isostere of thymidine (T) (*8*). In a DNA double helix, dF is destabilizing due to lack of hydrogen bonds. It is, however, more hydrophobic and stacks more favorably than thymidine (*9*). An NMR solution structure of a DNA dodecamer containing dF○A pairs revealed no significant deviations from B-form geometry (*10*). A canonical T-A base pair and the corresponding F○A pair are shown in Figure 1. dFTP serves as a substrate for *Escherichia coli* DNA polymerase and is inserted into a template opposite adenosine (A) with an efficiency 40-fold lower than that of dTTP, but with selectivity nearly as high as that observed for dTTP (*8, 11*). Replication of dF-containing templates occurs in bacterial cells with high fidelity (*12*).

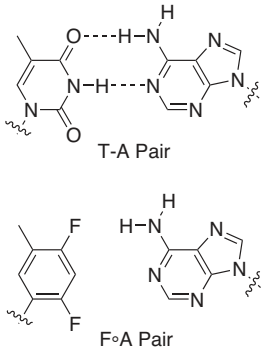

Figure 1. A canonical T-A base pair and the corresponding F°A pair.

Kool rationalized that hydrogen bonds are less important, and nucleotide shape is more important, in the fidelity of DNA replication than originally believed. (*12*)

We have evaluated the effects of the ribonucleotide analogue of 2,4-difluorotoluyl (rF) on *in vitro* RISC-mediated gene silencing activity of small interfering RNAs (siRNAs). Also reported is an evaluation of the thermal stability of duplexes containing the rF modification and a high-resolution crystal structure of a self-complementary 12-mer RNA duplex containing two rF°A pairs. A guide strand with an rF opposite to the cleavage site on the mRNA target directed cleavage of the mRNA at the predicted site. This experiment demonstrated the importance of stacking interactions rather than hydrogen bonding at this critical functional site. The biostability of siRNA duplex in serum is critical to therapeutic utility. The rF modification provided resistance to endonuclease cleavage, the first example of an induced stability that may be due to the hydration around the modification revealed by the crystal structure.

RESULTS AND DISCUSSION

The rF monomer was synthesized as described in Methods (Figure 2). In general, the thermal stability of a duplex is increased when C-5 of a pyrimidine has a methyl group as compared to a hydrogen (*13*); thus, we chose to evaluate the fluorine-substituted analogue of thymidine, rather than the uridine (U). Parsch and Engels reported a similar synthesis of a phosphoramide of 2,4-difluorobenzene riboside and its incorporation to a 12-mer RNA (*14*). The siRNA duplexes (Table 1) were synthesized using standard RNA oligonucleotide synthesis and purification protocols (*15, 16*). Thermal melting profiles of the RNA duplexes were used to evaluate the effect of the rF modification on RNA duplex stability (Table 1). The rF°A pair lowered the melting temperature (T_m), but was slightly less destabilizing than the mismatches tested. For example, the fully complementary duplex had a T_m of 73 °C. Substitution

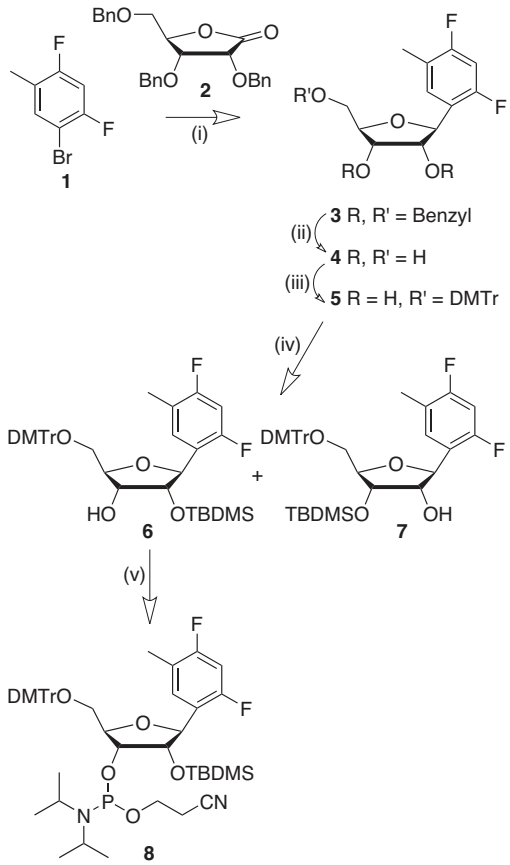

Figure 2. Scheme for the synthesis of ribo-difluorotoluyl nucleoside phosphoramidite (8). (i) *n*-BuLi/THF, −78 °C, 3 h, Ar atm, then 0 °C, 3 h; $Et_3SiH–BF_3{\cdot}Et_2O/CH_2Cl_2$, −78 °C to RT, 16 h, Ar atm., 81%; (ii) BCl_3/CH_2Cl_2, −78 to −40 °C, 4 h , Ar atm., 74%; (iii) DMTr-Cl, DMAP/Py, RT, 20 h, 71%; (iv) $AgNO_3$, Py, TBDMS-Cl/THF, RT, 12 h, 85% (combined, 6:7 2:8); (v) *i*-$Pr_2NP(Cl)O(CH_2)_2CN$, DMAP, *i*-Pr_2NEt/CH_2Cl_2, RT, Ar atm, 91%.

of rF for U at position 10 on the guide strand of duplex I (Table 1, duplex VII) decreased the T_m by 5.5 °C relative to the unmodified duplex, whereas substitution of cytidine (C) for U (Table 1, duplex X) lowered the T_m by 6.5 °C. Substitution with either purine lowered the T_m by 7.5 °C. Substitution of U with ribo 2,4-difluorobenzene nucleoside in a 12-mer RNA duplex decreases the thermal stability of the duplex by 10 °C (*14*). Though a direct comparison of thermal stability of a 19-mer duplex with two T overhangs on either end (Table 1, duplex VII) with a blunt-ended 12-mer duplex is difficult, the rF modification appears to be more stabilizing than the 2,4-difluorobenzene modification.

TABLE 1. siRNA duplex sequences, thermal stability, and biological activity

ID	Duplex sequence[a]	T_m(°C)[b]	IC_{50}(nM)[c]
I	CUUACGCUGAGUACUUCGATT TTGAAUGCGACUCAUGAAGCU	73	0.21
II	CUUACGCUGAGUACUUCGATT TTGAAUGCGACUCAUGAAGC**F**	nd	0.27
III	CUUACGCUGAGUACUUCGATT TTGAAUGCGACUCA**F**GAAGCU	nd	0.27
IV	CUUACGCUGAGUACUUCGATT TTGAA**F**GCGACUCAUGAAGCU	nd	0.58
V	CUUACGCUGAGUACUUCGATT TTGAAUGCGACU**F**AUGAAGCU	nd	>30
VI	CUUACGCUGAGUACUUCGATT TTGAAUGCGA**F**UCAUGAAGCU	nd	>30
VII	CUUACGCUGAGUACUUCGATT TTGAAUGCGAC**F**CAUGAAGCU	67.5	1.2
VIII	CUUACGCUGAGUACUUCGATT TTGAAUGCGAC**A**CAUGAAGCU	65.5	>30
IX	CUUACGCUGAGUACUUCGATT TTGAAUGCGAC**G**CAUGAAGCU	65.5	>30
X	CUUACGCUGAGUACUUCGATT TTGAAUGCGAC**C**CAUGAAGCU	66.5	0.92

[a]siRNA duplexes are shown with the sense strand above (written 5′ to 3′) and the guide strand below (written 3′ to 5′). All nucleotides were ribo with the exception of deoxythymidines (indicated by T). The rF modification is indicated by an **F**. [b]T_m is the midpoint of the thermal melting transition ±0.5 °C; nd indicates not determined. [c]The IC_{50} value is for luciferase silencing in HeLa cells.

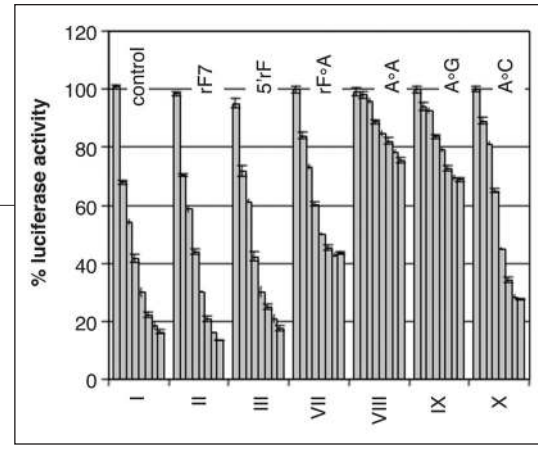

Figure 3. Effect of the rF modification vs mismatches on siRNA activity. siRNA duplexes targeted luciferase mRNA. siRNA activity was observed as a decrease in percent luciferase luminescence over concentrations ranging from 0.4 to 30 nM. Firefly/*Renilla* luciferase expression ratios were used to determine percent gene silencing relative to untreated controls

Modified siRNAs II–VII (Table 1) have guide strands complementary to firefly luciferase. These modified siRNAs were compared with unmodified control siRNA (Table 1, duplex I) for the ability to silence luciferase activity *in vitro*. The 50% inhibitory concentrations (IC_{50}) for duplexes tested are listed in Table 1, and selected data is shown in Figure. 3. When the rF was positioned at the 5′-end of the guide strand (Table 1, duplex II), silencing efficiency was similar to that observed with an unmodified duplex. When rF was substituted for U at position 7 (Table 1, duplex III), silencing was essentially the same as that of unmodified control (Table 1, duplex I). Activity of the duplex with rF at position 16 (Table 1, duplex IV) was reduced by approximately 2-fold compared with control. Substitution of rF for C near the center of the duplex was not tolerated (Table 1, duplexes V and VI). Interestingly, rF or C could be substituted for uridine at position 10 (Table 1, duplexes VII and X) without much loss of activity, but purine substitution at this position was not tolerated (Table 1, duplexes VIII and IX). In agreement with previous reports (*6, 7*), the effect of mismatches on silencing depends on the mismatch position, the sequence surrounding and opposite the mismatch, and the geometry of the mismatch, independent of whether the nucleobase is canonical or noncanonical.

The RISC mechanism requires 5′-phosphorylation for recruitment of the guide strand and the guide strand-targeted endonuclease (*argonaute2*) cleavage of the target mRNA (*17*). Previous work has shown that chemically modified siRNAs that cannot be 5′-phosphorylated at the guide strand are inactive (*18, 19*). The guide strand containing a 5′-rF modification was efficiently labeled with 5-[γ-^{32}P]ATP by T4 polynucleotide kinase (Figure 4) and was effective in the *in vitro* silencing assay (Figure 3).

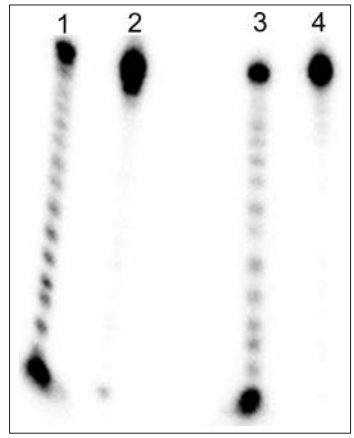

Figure 4. Phosphorylation of an oligonucleotide with a 5′ rF modification: lane 1, alkaline hydrolysis of 5′-^{32}P-end labeled unmodified guide strand of duplex I (Table 1); lane 2, reaction of unmodified guide strand of duplex I with 5-[γ-^{32}P]ATP and T4 polynucleotide kinase; lane 3, alkaline hydrolysis of 5′-^{32}P-end labeled 5′-rF-guide strand of duplex II (Table 1); lane 4, reaction of 5′-rF-guide strand with 5-[γ-^{32}P]ATP and T4 polynucleotide kinase. The guide strand of duplex II was labeled with ^{32}P by T4 polynucleotide kinase as efficiently as an unmodified oligonucleotide.

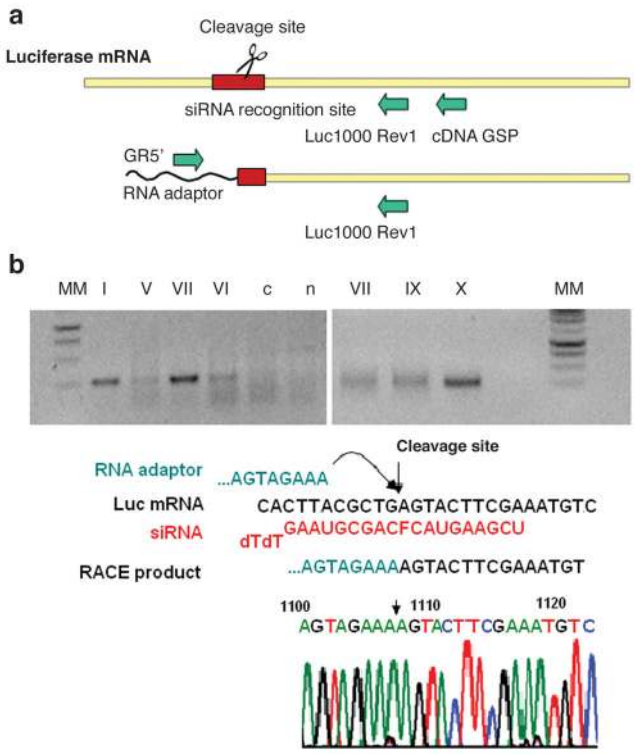

Figure 5. RACE analysis of cleavage products. a) Schematic representation of modified RACE analysis of siRNA-induced cleavage of luciferase mRNA. Primers used for amplification of cleavage products are indicated by the green arrows. b) Cells were treated with luciferase-targeting siRNA duplexes and RACE–PCR amplification products were analyzed using agarose gel electrophoresis. The lanes labeled MM are molecular weight markers, the lane labeled c indicates cells transfected with unrelated siRNA, n indicates cells alone. The cleavage site was verified by sequencing. The arrow on the chromatogram indicates the precise cleavage site where the RNA adaptor was ligated.

In a 21-mer siRNA duplex with mRNA, the cleavage site on the mRNA is located between nucleotides 10 and 11 from the 5′-end of the guide strand (*20, 21*). To insure that inhibition of luciferase expression observed with rF-modified siRNAs was due to siRNA-directed cleavage, specific mRNA cleavage products were characterized using a modified 5′-RACE (rapid amplification of cDNA ends) technique as previously described (*23–25*) (Figure 5). Sequencing of the PCR products demonstrated that siRNA-mediated cleavage occurred at the predicted site after treatment with the unmodified duplex as well as duplex VII (rF at position 10). No cleavage product was detected after treatment with duplex V (rF at position 9), in agreement with the results of the luciferase silencing assay (Table 1, Figure 3). Some product was observed after treatment with duplex VI, with rF substituted for C at position 11. No luciferase activity was detected in the expression assay with duplex VI; the discrepancy was most likely due to the higher sensitivity of the RACE assay. No cleavage product was observed in cells treated with unrelated siRNA or cells alone.

The biostability of siRNA duplex in serum is critical to therapeutic utility. The rF modification provides resistance to endonuclease cleavage (Figure 6). In this experiment, duplexes labeled at the 5′-end of one strand were incubated in human serum and the endonuclease cleavages were visualized by PAGE. The cleavage observed in the control unmodified duplex between U_{16} and A_{17} near the 3′-end was not observed in the rF-modified strand. Our data suggest that the rF modification increases the resistance to endonuclease activity of an siRNA without compromising silencing activity. Two other sites, U7 and C11, were cleaved by endonuclease and serve as internal controls for cleavage at the modified residue. The modified strand also undergoes degradation by exonucleases. In summary, whereas endonuclease cleavage occurred at U7 and C11, the modified site 16 was resistant.

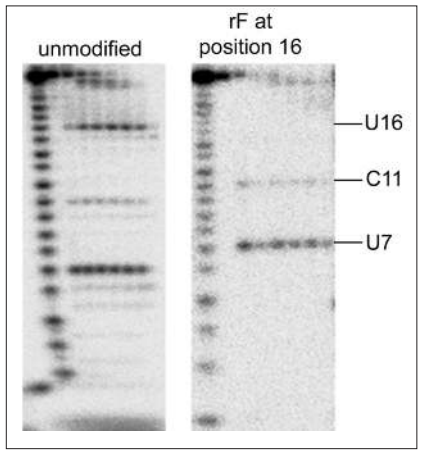

Figure 6. The rF modification imparted resistance to endonuclease cleavage to an siRNA duplex. The guide strand (5′-UCGAAGUACUCAGCGFAAGdTdT-3′) contained rF at position 16. The first panel shows the unmodified control siRNA. The second panel shows the rF-modified duplex IV. The positions of the observed endonuclease cleavages after U7, C11, and U16 (or rF16) are labeled. The first lane in each panel is alkaline hydrolysis of the labeled guide strand. The second lane was the duplex incubated in phosphate-buffered saline for 240 min. The subsequent lanes show cleavage observed after incubation for 0, 15, 30, 60, 120, and 240 min in 90% human serum.

To visualize the geometry of the rF◦A pair in an RNA duplex, we determined the crystal structure of the self-complementary duplex with two rF◦A pairs, 5′-CGCFAAUUAGCG-3′, to 1.61 Å resolution (residues of

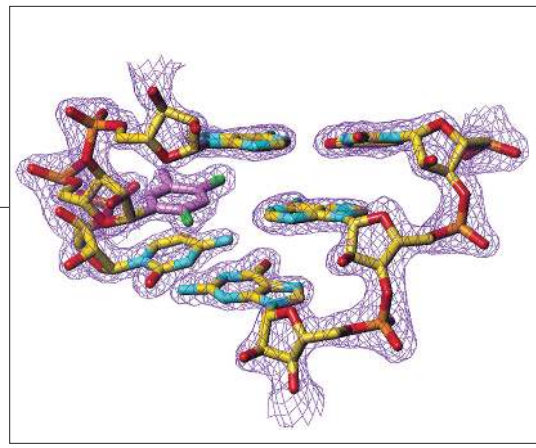

Figure 7. Example of the electron density in the region of the rF modification. Fourier ($2F_o - F_c$) sum electron density around the final structure in the region of the rF4∘A21 pair. Carbon atoms of the rF moiety are highlighted in magenta and fluorine atoms in green.

strands 1 and 2 are numbered 1–12 and 13–24, respectively). The structure of an RNA duplex of similar sequence, (5′-CGCgAAUUaGCG-3′)$_2$, with two guanosine∘adenosine (G∘A) mismatch pairs (underlined) was determined a decade ago (*26*). Recently, we collected diffraction data to better than 1.1 Å resolution for crystals of the dodecamer containing G∘A mismatches, and it was anticipated that replacement of G4 by rF and the formation of two rF∘A pairs would not hamper crystallization (Figure 7). In the duplex, the rF and A moieties are more than 0.8 Å apart, on average, along the long dimension of the pair (Figure 8, panels a and b) relative to the positions of bases in the central U-A pairs (Figure 8, panel c) as a consequence of the loss of hydrogen bonds and the C–H···N interaction in the rF∘A pair. The F4 of rF and the exocyclic N6 of A are at approximately the sum of their van der Waals radii. This leads to an opening of rF∘A pairs (of 10°) compared to a U-A pair and a local widening of the major groove. Other structural changes include a marked roll between rF16 and A17 (–20°) and strong shearing in the rF16∘A9 pair, with the rF moiety shifted 0.75 Å into the major groove relative to other base pairs (Figure 8, panel b). The same pair also exhibited a very strong propeller twist (–30°; –13° in the rF4∘A21 pair; average value in the duplex, –17°). Unlike O2 and O4 of U, fluorine atoms in rF residues do not engage in hydrogen bonds to water molecules, and there was an absence of a well-ordered water structure around difluorotoluyl moieties in both grooves.

Chemical modification of siRNA is required for therapeutic applications due to insufficient chemical stability and resistance to nuclease degradation of unmodified RNA and inefficient uptake of the siRNA into mammalian cells. Although there are virtually no technical limitations regarding chemical modification of the nucleobase, sugar, and phosphate, extensive interactions of siRNA with protein factors put constraints on the types of modifications and the number of residues that can be modified without severely impairing the efficacy of the siRNA. We have synthesized and evaluated siRNA duplexes modified with the ribonucleotide analogue of 2,4-difluorotoluyl (rF). Difluorotoluyl was first synthesized and evaluated in the context of DNA duplexes by Kool and co-workers (*8*). The dF modification destabilizes DNA duplexes but is accepted by DNA polymerase with high fidelity (*12*).

In the fidelity of DNA polymerase, nucleotide shape appears to be more important than hydrogen bonding, as selectivity for the dF analogue is roughly equivalent to that of T (*12*). Our results suggest that hydrogen bonds are not as critical as shape in selectivity of siRNA-mediated RISC cleavage. Whereas substitution of either A or G was not tolerated in the guide strand opposite the cleavage site, neither rF nor C abolished silencing of luciferase in an expression assay (Figure 3, Table 1). A RACE assay was used to ensure that the mechanism of silencing was not altered by rF substitution (Figure 5, panel b). When rF replaced C at position 9 (Table 1,

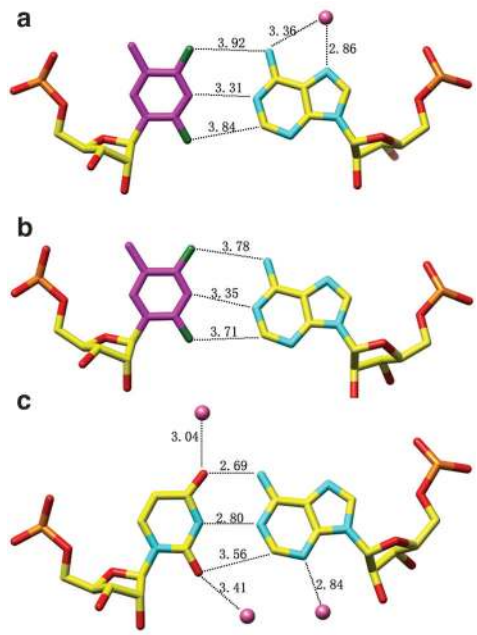

Figure 8. Geometry and hydration of rF∘A and U-A base pairs in the RNA dodecamer duplex. Base pairs (a) rF4∘A21, (b) rF16∘A9, and (c) A6-U19 are shown. Atoms are colored yellow, red, cyan, and orange for carbon, oxygen, nitrogen, and phosphorus, respectively. Carbon atoms of the difluorotoluene moiety are highlighted in magenta, fluorine atoms are green and water molecules are pink. Selected hydrogen bonds in the U-A base pair and the corresponding interactions in the rF∘A pair are shown as dashed lines with distances in angstroms. The lengths of Watson–Crick hydrogen bonds and the O2(U) to C2(A) distance shown in panel c are average values based on the four central U-A pairs. In panel c, the water molecules hydrogen bonded to O2(U) and N3(A) are separated by 3.6 Å. The figures were generated with the program UCSF Chimera (*26*).

duplex V), no cleavage product was observed. An rF substitution at position 10 reduced silencing by about 6-fold compared to the unmodified siRNA, but a RACE product was observed and, as shown by sequencing of the product (data not shown), had the sequence expected for cleavage opposite positions 10 and 11 of the guide strand. To our knowledge, this is the first demonstration of RNA-mediated gene silencing using an siRNA chemically modified at the cleavage site with a nucleobase mimetic that does not form a Watson-Crick base pair.

The crystal structure of a duplex containing two rFoA pairs indicates that the presence of an isolated rFoA pair leads to a host of local changes that subtly affect the geometry of the duplex both geometrically and thermodynamically compared to a duplex with canonical U-A pairs. In particular, local stacking interactions and water structure undergo changes relative to a Watson-Crick-paired duplex. On the basis of the structural and thermodynamic data, one can conclude that the duplex is not as rigid at the sites of rF incorporation as it would be if a Watson-Crick pair was present, consistent with the observations from a recent molecular dynamics simulation (*27*). In spite of these structural variations, the retention of silencing activity, recognition by the RISC enzymes and kinase, and improved endonuclease resistance in serum all warrant further evaluation of rF in therapeutic siRNAs.

METHODS

Synthesis of Ribo-difluorotoluyl Nucleoside Phosphoramidite. The difluorotoluyl (rF) monomer **8** was synthesized as shown in Figure 2.

1. 2,3,5-Tri-*O*-benzyl-1-C-(2,4-difluorotoluene)-D-β-riboside (3). Compound **1** was prepared according to Kool's procedure (*28*). *n*-Butyl lithium (4.25 mL, 2.5 M in hexanes) was added to a cold solution of 5-bromo-2,4-difluorotoluene (2.19 g, 10.63 mmol) in anhydrous THF (50 mL) at −78 °C and stirred at the same temperature for 3 h under an argon atmosphere. 2,3,5-Tri-*O*-benzyl-D-ribolactone (**2**, 4.45 g, 10.63 mmol) in dry THF (17 mL) was added dropwise to the above solution and stirred at −78 °C for 2 h and then at 0 °C for 3 h. The reaction mixture was quenched with saturated $NaHCO_3$ solution and extracted with dichloromethane (3 × 120 mL). The organic phase was washed with saturated aqueous $NaHCO_3$ solution and brine, dried (Na_2SO_4), and concentrated to a crude residue that was dried under high vacuum for 1.5 h. $BF_3{\circ}Et_2O$ (4 mL) and Et_3SiH (5.1 mL) were added to a cold solution of the crude residue in anhydrous dichloromethane (80 mL) at −78 °C and stirred at −78 °C to ambient temperature under argon overnight. The reaction was quenched by addition of 1 N HCl, stirred at ambient temperature for 1 h, and subsequently neutralized with 1 N aqueous NaOH solution. The product was extracted into dichloromethane (3 × 100 mL), washed with saturated aqueous $NaHCO_3$ solution and then brine, dried over Na_2SO_4, and concentrated to a crude residue that was applied to a column of silica gel and eluted with hexanes–ethyl acetate (4:1) to give pure compound **3** (4.57 g, 81%) as a syrup. Characterization of the product by NMR is described in Supporting Information.

2. 1-C-(2,4-Difluorotoluene)-D-β-riboside (4). BCl_3 (31 mL, 1 M in dichloromethane) was added to a cold solution of 2,3,5-tri-*O*-benzyl-1-C-(2,4-difluorotoluene)-D-β-riboside **3** (1.1 g, 2.08 mmol) in anhydrous dichloromethane (100 mL) at −78 °C under an argon atmosphere. The reaction mixture was stirred at −78 °C for 2.5 h and at −45 °C for 1 h. The reaction was quenched with dichloromethane–methanol (50 mL, 1:1) and saturated ammonia–methanol solution. After concentration to a crude residue, the solution was applied to a column of silica gel and eluted with dichloromethane–methanol (5:1) to give compound **4** (400 mg, 74%) as a white solid. Characterization of the product by NMR is described in Supporting Information.

3. 5′-*O*-(4,4′-Dimethoxitrityl)-1-C-(2,4-difluorotoluene)-D-β-riboside (5). 4,4′-Dimethoxtrityl chloride (535 mg, 1.58 mmol) was added to a solution of 1-C-(2,4-difluorotoluene)-D-β-riboside **4** (370 mg, 1.42 mmol) in anhydrous pyridine (3 mL) in the presence of 4-*N*,*N*-dimethylaminopyridine (DMAP, 40 mg) and stirred at ambient temperature under argon overnight. The reaction mixture was concentrated to a crude residue and co-evaporated with dry toluene (3 × 10 mL). The crude residue was applied to a column of silica gel saturated with 2% triethylamine in hexanes and eluted with hexanes–ethyl acetate (1.5:1) to give pure compound **5** (570 mg, 71%) as an amorphous white solid. Characterization of the product by NMR is described in Supporting Information.

4. 5′-*O*-(4,4′-Dimethoxitrityl)-2′-*O*-(*tert*-butyldimethylsilyl)-1-C-(2,4-difluorotoluene)-D-β-riboside (6). Anhydrous pyridine (907 μL) and $AgNO_3$ (235 mg, 1.35 mmol) were added to a solution of 5′-*O*-(4,4′-dimethoxitrityl)-1-C-(2,4-difluorotoluene)-D-β-riboside **5** (640 mg, 1.14 mmol) in anhydrous THF (8 mL), and the solution was stirred at ambient temperature for 20 min under argon atmosphere. *tert*-Butyldimethylsilyl chloride (235 mg, 1.48 mmol) in dry THF (3 mL) was added to the stirring mixture, and stirring was continued at ambient temperature for 3 h. Solids were filtered off, and the filtrate was concentrated to a crude residue that was applied to a column of silica gel and then eluted with hexane–Et_2O (4:1) to give compound **6** (360 mg, 46%), compound **7** (5′-*O*-(4,4′-dimethoxitrityl)-3′-*O*-(*tert*-butyldimethylsilyl)-1-C-(2,4-difluorotoluene)-D-β-riboside, 40 mg, 5%), and a mixture of compounds **6** and **7** (650 mg) as amorphous solid. Characterization of the product by NMR is described in Supporting Information.

5. 5′-*O*-(4,4′-Dimethoxitrityl)-2′-*O*-(*tert*-butyldimethylsilyl)-1′-C-(2,4-difluorotoluene)-D-riboside-3′-*O*-caynoethyl-*N*,*N*-di isopropylphosphoramidate (8). 2-Cyanoethyl-*N*,*N*-diisopropyl-chlorophosphoramidite (252 mg,1.07 mmol) was added to a solution of 5′-*O*-(4,4′-dimethoxitrityl)-2′-*O*-(*tert*-butyldimethylsilyl)-1-C-(2,4-difluorotoluene)-D-β-riboside **6** (360 mg, 0.53 mmol), diisopropylethylamine (504 μL, 2.93 mmol), and DMAP (19 mg) in anhydrous dichloromethane (6 mL) and stirred at ambient temperature for 6 h under argon. The reaction mixture was concentrated to a crude residue, applied to a column of silica gel that was saturated with 2% triethylamine in hexanes, and eluted with hexanes–ethyl acetate (2:1) to give pure compound **8** (420 mg, 91%) as an amorphous white solid. Characterization of the product by NMR is described in Supporting Information.

Oligonucleotide Synthesis. The RNA molecules were synthesized on a 394 ABI synthesizer using the manufacturer's standard 93 step cycle with modifications described below. The dT-controlled pore glass (CPG) was prepacked, 1 μmol, 500 Å from Proligo Biochemie GmbH. RNA phosphoramidites with fast deprotecting groups were obtained from Pierce Nucleic Acid Technologies or were synthesized as described above and were used at concentrations of 0.15 M in CH_3CN unless otherwise stated. Specifically, in addition to the rF amidite **8**, 3′-*O*-(2-cyanoethyl)-*N*,*N*′-diisopropyl)-phosphoramidites of 5′-O-(4,4′-dimethoxytrityl)-2′-*O*-*t*-butyldimethylsilyl-N^6-phenoxyacetyladenosine, 5′-*O*-(4,4′-dimethoxytrityl)-2′-*O*-*t*-butyldimethylsilyl-N^2-*p*-isopropylphenoxyacetylguanosine, 5′-*O*-(4,4′-dimethoxytrityl)-2′-*O*-*t*-butyldimethylsilyl-N^4-acetylcytidine, 5′-*O*-(4,4′-dimethoxytrityl)-2′-*O*-*t*-butyldimethylsilyluridine, and 5′-*O*-(4,4′-dimethoxytrityl)thymidine were used for the oligonucleotide synthesis.

The coupling times were 7.5 min for the RNA monomers and 10 min for the rF monomer. Details of other reagents were as follows: activator, 5-(ethylthio)-1*H*-tetrazole (0.25 M); Cap A, 5% phenoxyacetic anhydride/THF/pyridine; Cap B, 10% *N*-methylimidazole/THF; PO-oxidation, 0.02 M iodine in THF/water/pyridine. Detritylation was achieved with 3% TCA/dichloromethane.

The oligonucleotide was cleaved from the CPG, with simultaneous deprotection of base and phosphate groups, with 1.0 mL of a mixture of ethanolic ammonia (ammonia–ethanol, 3:1) for 16 h at 55 °C. The solution was decanted, lyophilized, and resuspended in 0.2 mL of triethylamine trihydrofluoride (TEA.3HF, Aldrich) and was incubated at 65 °C for 90 min to remove the *t*-butyldimethylsilyl (TBDMS) groups. The completely deprotected oligonucleotides were then precipitated from anhydrous methanol (MeOH, 0.4 mL).

The oligonucleotides were purified by vertical slab polyacrylamide gel electrophoresis (PAGE), generally 20% (w/v) acrylamide and 5% BIS (with respect to the mass of acrylamide). About 50 ODs were typically loaded onto preparative gels in the loading buffer of 80% formamide in 10× Tris-borate-EDTA buffer (TBE). The desired bands were excised and shaken overnight in 5 mL of 100 mM sodium acetate. The extracted oligonucleotides were desalted using C-18 Sep-Pak cartridges (Waters). The oligonucleotides were characterized by electrospray mass spectroscopy (ES/MS) and analytical anion-exchange HPLC and/or capillary gel electrophoresis (CGE). The LC-MS data for single strands are listed in Supplementary Table 1 in Supporting Information.

Thermal Denaturation (T_m) Studies. Molar extinction coefficients for the oligonucleotides were calculated according to nearest-neighbor approximations (units = 10^4 M^{-1} cm^{-1}). Duplexes were prepared by dissolving lyophilized equimolar amounts of the complementary strands in phosphate-buffered saline (pH 7.0) to give a final concentration of 2.4 μM of each strand. The solutions were heated to 90 °C for 10 min and cooled slowly to room temperature before measurements. Prior to analysis, samples were degassed by placing them in a speed-vac concentrator for 2 min. Denaturation curves were acquired at 260 nm at a rate of heating of 0.5 °C min^{-1} using a Varian CARY spectrophotometer fitted with a 12-sample thermostated cell block and a temperature controller.

***In Vitro* Analysis of Luciferase Expression.** HeLa cells that stably express both firefly and *Renilla* luciferase (HeLa Dual-luc cells) were grown at 37 °C in Eagle medium supplemented with 10% fetal bovine serum (FBS), 100 units mL^{-1} penicillin, 100 μg mL^{-1} streptomycin, 0.5 μg mL^{-1} puromycin, and 500 μg mL^{-1} zeocin (Invitrogen). Cells were passaged regularly to maintain exponential growth. Twenty-four hours prior to siRNA transfection, cells were seeded on opaque, white 96-well plates (Costar) at a concentration of 15000 cells per well in antibiotic-free, phenol red-free DMEM (Invitrogen).

In vitro activity of siRNAs was determined using a high-throughput 96-well plate format assay for luciferase activity. HeLa Dual-luc cells were transfected with firefly luciferase targeting siRNAs at concentrations ranging from 0.40–30 nM using Lipofectamine 2000 (Invitrogen) according to the manufacturer's protocol. After 24 h, cells were analyzed for both firefly and *Renilla* luciferase expression using a plate luminometer (VICTOR^2, PerkinElmer) and the Dual-Glo Luciferase Assay kit (Promega). Firefly/*Renilla* luciferase expression ratios were used to determine the percentage of gene silencing relative to untreated controls.

***In Vitro* 5′-Phosphorylation.** Oligonucleotides with (Table 1, guide strand of duplex II) and without (Table 1, guide strand of duplex I) the rF modification at the 5′-end were incubated with [^{32}P]ATP and T4 polynucleotide kinase using standard conditions and analyzed by denaturing 20% polyacrylamide gel electrophoresis.

RACE Analysis. HeLa-Dual Luc cells were transfected with 30 nM of the indicated siRNA at a density of 500 000 cells per well in a six-well plate using Lipofectamine 2000 transfection reagent (Invitrogen). Twenty-four hours post-transfection, cells were harvested, and total RNA was isolated using Qiagen's RNeasy kit (Qiagen). One microgram of total RNA was subjected to RACE assay for detection of 3′ cleavage fragments (GeneRacer, Invitrogen). The GeneRacer RNA adaptor was ligated directly to untreated total RNA following the manufacturer's protocol. cDNA was generated using a gene-specific primer (cDNA GSP, 5′-TGTACATCGACTGAAATCCCTGGT-3′). To detect cleavage products, PCR was performed using primers complementary to the RNA adaptor (GR5′, 5-′CTCTAGAGCGACTGGAGCACGAGGACACTA-3′, and Luc 1000 Rev1, 5′-GGAAACGAACACCACGGTAGGCT-3′). Amplification products were resolved by agarose gel electrophoresis and visualized by ethidium bromide staining. The identity of specific PCR products was confirmed by sequencing.

Crystallization and Structure Determination. Crystals of the rF-modified RNA dodecamer were grown at 18 °C by the hanging-drop vapor diffusion method, using the Nucleic Acid Miniscreen (Hampton Research) (*29*). Droplets containing 0.5 mM oligonucleotide, 5% 2′-methyl-2,4-pentanediol (MPD), 20 mM sodium cacodylate, pH 5.5, 10 mM cobalt hexamine, 20 mM LiCl, and 10 mM $MgCl_2$ were equilibrated against a reservoir of 35% MPD. Crystals appeared after 1 week. Crystals of the rF-modified RNA dodecamer grew readily but exhibited a different space group and packing than the duplex without the rF substitution. Diffraction data were collected at 120 K on the insertion device beamline (5-ID) of the DuPont–Northwestern–Dow Collaborative Access Team (DND-CAT) at the Advanced Photon Source (APS), Argonne, IL. Data were processed with the program X-GEN (*30*), and the structure was determined by the Molecular Replacement method using the program EPMR (*31*). Refinement of the structure was carried out with the programs CNS and REFMAC (*32, 33*). The geometry of the RNA duplex was analyzed with the program CURVES (Version 5.3) (*34*). Selected crystal data and refinement parameters are listed in Supplementary Table 2 in Supporting Information.

Accession Codes. Structure factors and final coordinates have been deposited in the RCSB Protein Data Bank with ID code 2G92.

Acknowledgment: We thank C. Wilds, Z. Wawrzak, and G. Lavine for their valuable contributions. Support from the U.S. National Institutes of Health is gratefully acknowledged (GM55237 to M.E.). Use of the Advanced Photon Source was supported by the U.S. Department of Energy, Basic Energy Sciences, Office of Science, under

Contract No. W-31-109-Eng-38. The DuPont-Northwestern-Dow Collaborative Access Team (DND-CAT) Synchrotron Research Center at the Advanced Photon Source (Sector 5) is supported by E. I. DuPont de Nemours & Co., The Dow Chemical Company, the National Science Foundation, and the State of Illinois.

Supporting Information Available: This material is available free of charge via the Internet.

REFERENCES

1. Novina, C. D., and Sharp, P. A. (2004) The RNAi revolution, *Nature 430*, 161–164.
2. Mello, C. C., and Conte, D. (2004) Revealing the world of RNA interference, *Nature 431*, 338–342.
3. Hannon, G. J., and Rossi, J. J. (2004) Unlocking the potential of the human genome with RNA interference, *Nature 431*, 371–378.
4. Tuschl, T., and Borkhardt, A. (2002) Small interfering RNAs: a revolutionary tool for the analysis of gene function and gene therapy, *Mol. Interventions 2*, 158–167.
5. Manoharan, M. (2004) RNA interference and chemically modified small interfering RNAs, *Curr. Opin. Chem. Biol. 8*, 570–579.
6. Dorsett, Y., and Tuschl, T. (2004) siRNAs: applications in functional genomics and potential as therapeutics, *Nat. Rev. Drug Discovery 3*, 318–329.
7. Kurreck, J. (2003) Antisense technologies. Improvement through novel chemical modifications, *Eur. J. Biochem. 270*, 1628–1644.
8. Moran, S., Ren, R. X., and Kool, E. T. (1997) A thymidine triphosphate shape analog lacking Watson–Crick pairing ability is replicated with high sequence selectivity, *Proc. Natl. Acad. Sci. U.S.A. 94*, 10506–10511.
9. Guckian, K. M., Schweitzer, B. A., Ren, R. X., Sheils, C., Paris, P. L., Tahmassebi, D. C., and Kool E. T. (1996) Experimental Measurement of Aromatic Stacking Affinities in the Context of Duplex DNA, *J. Am. Chem. Soc. 118*, 8182–8183.
10. Guckian, K. M., Krugh, T. R., and Kool, E. T. (1998) Solution structure of a DNA duplex containing a replicable difluorotoluene–adenine pair, *Nat. Struct. Biol. 5*, 954–959.
11. Morales, J. C., and Kool, E. T. (1998) Efficient replication between non-hydrogen bonded nucleoside shape analogs, *Nat. Struct. Biol. 5*, 950–954.
12. Delaney, J. C., Henderson, P. T., Helquist, S. A., Morales, J. C., Essigmann, J. M., and Kool, E. T. (2003) High-fidelity *in vivo* replication of DNA base shape mimics without Watson–Crick hydrogen bonds. *Proc. Natl. Acad. Sci. U.S.A. 100*, 4469–4473.
13. Freier, S. M., and Altmann, K.-H. (1997) The ups and downs of nucleic acid duplex stability: structure–stability studies on chemically-modified DNA:RNA duplexes, *Nucleic Acids Res. 25*, 4429–4443.
14. Parsch, J., and Engels, J. W. (2000) Synthesis of fluorobenzene and benzimidazole nucleic-acid analogues and their influence on stability of RNA duplexes, *Helv. Chim. Acta 83*, 1791–1808.
15. Manoharan, M., Xia, J. and Rajeev, K. G. (2006) Single- and double-stranded oligonucleotides containing unnatural nucleobases for inhibition of gene expression and treatment of disease. U.S. Pat. Appl. Publ. 2006035254 A1 20060216 105 pp.
16. Rajeev, K. G., Xia, J., Noronha, A., Toudjarska, I., Li, F., Akinc, A., Frank-Kamenetsky, M., Braich, R., Egli, M. and Manoharan, M. (2006) RNA interference: RISC-mediated recognition of non-canonical ribo-difluorotoluyl nucleotide: Synthesis, structure and activity. Abstracts of Papers, 231st ACS National Meeting, Atlanta, GA, United States, March 26-30, 2006, CARB-066.
17. Meister, G., Landthaler, M., Patkaniowska, A., Dorsett, Y., Teng, G., and Tuschl, T. (2004) Human Argonaute2 mediates RNA cleavage targeted by miRNAs and siRNAs, *Mol. Cell 15*, 185–197.
18. Nykanen, A., Haley, B., and Zamore, P. D. (2001) ATP requirements and small interfering RNA structure in the RNA interference pathway, *Cell 107*, 309–321.
19. Schwarz, D. S., Hutvagner, G., Haley, B., and Zamore, P. D. (2002) Evidence that siRNAs function as guides, not primers, in the Drosophila and human RNAi pathways. *Mol. Cell 10*, 537–548.
20. Elbashir, S. M., Martinez, J., Patkaniowska, A., Lendeckel, W., and Tuschl, T. (2001) Functional anatomy of siRNAs for mediating efficient RNAi in Drosophila melanogaster embryo lysate, *EMBO J. 20*, 6877–6888.
21. Harborth, J., Elbashir, S. M., Vandenburgh, K., Manninga, H., Scaringe, S. A., Weber, K., and Tuschl, T. (2003) Sequence, chemical, and structural variation of small interfering RNAs and short hairpin RNAs and the effect on mammalian gene silencing, *Antisense Nucleic Acid Drug Dev. 13*, 83–105.
22. Llave, C., Xie, Z., Kasschau, K. D., and Carrington, J. C. (2002) Cleavage of Scarecrow-like mRNA targets directed by a class of Arabidopsis miRNA, *Science 20*, 2053–2056.
23. Yekta, S., Shih, I. H., and Bartel, D. P. (2004) MicroRNA-directed cleavage of HOXB8 mRNA, *Science 304*, 594–596.
24. Soutschek, J.; Akinc, A.; Bramlage, B.; Charisse, K.; Constien, R.; Donoghue, M.; Elbashir, S.; Geick, A.; Hadwiger, P.; Harborth, J.; John, M.; Kesavan, V.; Lavine, G.; Pandey, R. K.; Racie, T.; Rajeev, K. G.; Roehl, I.; Toudjarska, I.; Wang, G.; Wuschko, S.; Bumcrot, D.; Koteliansky, V.; Limmer, S.; Manoharan, M.; Vornlocher, H.-P. (2004) Therapeutic silencing of an endogenous gene by systemic administration of modified siRNAs, *Nature 432*, 173–178.
25. Leonard, G. A., McAuley-Hecht, K. E., Ebel, S., Lough. D. M., Brown, T. and Hunter, W. N. (1994) Crystal and molecular structure of r(CGCGAAUUAGCG): an RNA duplex containing two G(anti). A(anti) base pairs, *Structures 2*, 483–494.
26. Pettersen, E. F., Goddard, T. D., Huang, C. C., Couch, G. S., Greenblatt, D. M., Meng, E. C., and Ferrin, T. E. (2004) UCSF Chimera—A visualization system for exploratory research and analysis, *J. Comput. Chem. 25*, 1605–1612.
27. Zacharias, M., and Engels, J. W. (2004) Influence of a fluorobenzene nucleobase analogue on the conformational flexibility of RNA studied by molecular dynamics simulations, *Nucleic Acids Res. 32*, 6304–6311.
28. Schweitzer, B. A., and Kool, E. T. (1994) Nonpolar Aromatic Nucleosides as Hydrophobic Isosteres of DNA Nucleosides, *J. Org. Chem. 59*, 7238–7242.
29. Berger, I., Kang, C. H., Sinha, N., Wolters, M., and Rich, A. A. (1996) Highly Efficient 24-Condition Matrix for the Crystallization of Nucleic Acid Fragments, *Acta Crystallogr., Sect. D: Biol. Crystallogr. 52*, 465–468.
30. Howard, A. J. (2000) Data processing in macromolecular crystallography, in *Crystallographic Computing 7. Proceedings from the Macromolecular Crystallographic Computing School* (Bourne, P. E., Watenpaugh, K. D., Eds.), pp 150–165, Oxford University Press, Oxford, U.K.
31. Kissinger, C. R., Gehlhaar, D. K., and Fogel, D. B. (1999) Rapid automated molecular replacement by evolutionary search, *Acta Crystallogr., Sect. D: Biol. Crystallogr. 55*, 484–491.
32. Brünger A. T., Adams, P. D., Clore, G. M., DeLano, W. L., Gros, P., Grosse-Kunstleve, R. W., Jiang, J.-S., Kuszewski, J., Nilges, M., Pannu, N. S., Read, R. J., Rice, L. M., Simonson, T., Warren, G. L. (1998) Crystallography & NMR system: A new software suite for macromolecular structure determination, *Acta Crystallogr., Sect. D: Biol. Crystallogr. 54*, 905–921.
33. Murshudov, G. N., Vagin, A. A., and Dodson, E. J. (1997) Refinement of macromolecular structures by the maximum-likelihood method, *Acta Crystallogr., Sect. D: Biol. Crystallogr. 53*, 240–255.
34. Lavery, R., and Sklenar, H. (1989) Defining the structure of irregular nucleic acids: conventions and principles, *J. Biomol. Struct. Dyn. 6*, 655–667.